OXFORD

ORIGINAL ARTICLE

Immunohistochemical Method and Histopathology Judging for the Systemic Synuclein Sampling Study (S4)

Thomas G. Beach, MD, PhD, Geidy E. Serrano, PhD, Thomas Kremer, PhD,
Marta Canamero, MD, PhD, Sebastian Dziadek, PhD, Hadassah Sade, PhD,
Pascal Derkinderen, MD, PhD, Anne-Gaëlle Corbillé, MD, Franck Letournel, MD, PhD,
David G. Munoz, MD, Charles L. White, III, MD, Julie Schneider, MD, MS, John F. Crary, MD, PhD,
Lucia I. Sue, BS, Charles H. Adler, MD, PhD, Michael J. Glass, BS, Anthony J. Intorcia, BS,
Jessica E. Walker, BS, Tatiana Foroud, PhD, Christopher S. Coffey, PhD, Dixie Ecklund, RN,
Holly Riss, BA, Jennifer Goßmann, Dr rer nat, Fatima König, MD, Catherine M. Kopil, PhD,
Vanessa Arnedo, MPH, Lindsey Riley, MPH, Carly Linder, MPH, Kuldip D. Dave, PhD,
Danna Jennings, MD, John Seibyl, MD, Brit Mollenhauer, MD, and Lana Chahine, MD, and
the Systemic Synuclein Sampling Study (S4)*

From the Civin Laboratory for Neuropathology, Banner Sun Health Research Institute, Sun City, Arizona (TGB, GES, LIS, MJG, AJI, JEW); Roche Pharmaceutical Research and Early Development, Roche Innovation Center Basel, F Hoffman-La Roche, Ltd. (TK, MC, SD, HS), Basel, Switzerland; Roche Pharma Research and Early Development, Roche Innovation Center (TK, MC, SD, HS), Munich, Penzberg, Germany; Department of Neurology, CHU Nantes, Inserm, U1235, Nantes University (PD, A-GC, FL), Nantes F-44035, France; CHU Angers, Neurobiology and Neuropathology Laboratory (PD, A-GC, FL), Angers F-49033, France; Laboratory Medicine and Keenan Research Centre for Biomedical Research of the Li Ka Shing Knowledge Institute, St. Michael's Hospital, University of Toronto, Toronto, ON, Canada (DGM); Department of Pathology, University of Texas Southwestern Medical Center, Dallas, Texas (CLW); Rush Alzheimer's Disease Center, Chicago, Illinois (JS); Department of Pathology, Fishberg Department of Neuroscience, Friedman Brain Institute, Ronald M. Loeb Center for Alzheimer's Disease, Icahn School of Medicine at Mount Sinai, New York, New York (JFC); Department of Neurology, Mayo Clinic Arizona, Scottsdale, Arizona (CHA); Indiana University School of Medicine, Indianapolis, Indiana (TF); Department of Biostatistics, University of Iowa, Iowa City, Iowa (CSC, DE, HR); Targos Molecular Pathology GmbH, Kassel, Germany (JG, FK); The Michael J. Fox Foundation for Parkinson's Research, New York, New York (CMK, VA, LR, KDD); Department of Neurology, University of Pennsylvania Perelman School of Medicine, Philadelphia, Pennsylvania (CL); Avid Radiopharmaceuticals, Philadelphia, Pennsylvania (DJ); Institute for Neurodegenerative Disorders, New Haven, Connecticut (JS); Paracelsus-Elena-Klinik, Kassel and University Medical Center Goettingen, Goettingen, Germany (BM); and Department of Neurology, University of Pittsburgh, Pittsburgh, Pennsylvania (LC).

Send correspondence to: Thomas G. Beach, MD, PhD, Civin Laboratory for Neuropathology, Banner Sun Health Research Institute, 10515 West Santa Fe Drive, Sun City, AZ 85351; E-mail: thomas.beach@bannerhealth.com

Thomas Beach has been paid as a consultant by Roche Diagnostics, whose immunohistochemical method is used in this study. Thomas Beach has received grant support and has been paid travel expenses from the Michael J. Fox Foundation, is paid as a consultant and/or has had travel paid, by Prothena Biosciences and Roche Diagnostics, and is doing contract research for Avid Radiopharmaceuticals, Navidea Biopharmaceuticals and Aprinoia Therapeutics. Geidy E. Serrano has no conflict of interest to declare. Thomas Kremer, Marta Canamero, Sebastian Dziadek, and Hadassah Sade are employees of F. Hoffmann-La Roche Ltd. Marta Canamero and Sebastian Dziadek own Roche stocks. Pascal Derkinderen, Anne-Gaëlle Corbillé, Franck Letournel, David Munoz, Charles White, and Julie Schneider have no conflicts of interest or no financial disclosures related to this study. John F. Crary and Lucia I. Sue have no conflict of interest related to this study. John F. Crary has received research support from Genentech/Roche. Lucia I. Sue has no financial disclosure. Charles Adler has no conflict of interest related to this study. Consulting in the past year: Extera Partners, Jazz, Lundbeck, Minerva, Neurocrine, Revance, Scion, Sunovion. Michael Glass, Anthony J. Intorcia, and Jessica E. Walker have no conflict of interest related to this study. Tatiana Foroud has no conflict of interest related to this study. Tatiana Foroud received funding from the National Institutes of Health (NIH), The Michael J. Fox Foundation, the US Department of Defense, San Diego State University, The University of Texas at Austin, and Waggoner Center for Alcohol/Addiction Research. Christopher S. Coffey has no conflict of interest related to this study. Christopher S. Coffey received research support from the Michael J. Fox Foundation. Dixie Ecklund has no conflict of interest related to this study. Dixie Ecklund received research support from the National Institute of Health and the Michael J. Fox Foundation. Holly Riss has no conflict of interest related to this study. Holly Riss received research support from the National Institute of Health and the Michael J. Fox Foundation. Jennifer Goßmann is an employee of Targos Molecular Pathology, Gmbh. Fatima König is an employee of Targos Molecular Pathology, Gmbh. Catherine M. Kopil is an employee of the Michael J. Fox Foundation. Vanessa Arnedo is an employee of the Michael J. Fox Foundation. Lindsey Riley is an employee of the Michael J. Fox Foundation. Carly Linder has no conflict of interest or no financial disclosures related to this study. Kuldip D. Dave is an employee of the Michael J. Fox Foundation. Danna Jennings is an employee of Denali Therapeutics. Danna Jennings is a minor share holder Eli Lilly and Co. John Seibyl has no conflict of interest to declare. John Seibyl has equity interest in Invicro and is a consultant to GE Healthcare, Piramal, Roche, and Biogen. Brit

Abstract

Immunohistochemical (IHC) α-synuclein (Asyn) pathology in peripheral biopsies may be a biomarker of Parkinson disease (PD). The multi-center Systemic Synuclein Sampling Study (S4) is evaluating IHC Asyn pathology within skin, colon and submandibular gland biopsies from 60 PD and 20 control subjects. Asyn pathology is being evaluated by a blinded panel of specially trained neuropathologists. Preliminary work assessed 2 candidate immunoperoxidase methods using a set of PD and control autopsy-derived sections from formalin-fixed, paraffin-embedded blocks of the 3 tissues. Both methods had 100% specificity; one, utilizing the 5C12 monoclonal antibody, was more sensitive in skin (67% vs 33%), and was chosen for further use in S4. Four trainee neuropathologists were trained to perform S4 histopathology readings; in subsequent testing, their scoring was compared to that of the trainer neuropathologist on both glass slides and digital images. Specificity and sensitivity were both close to 100% with all readers in all tissue types on both glass slides and digital images except for skin, where sensitivity averaged 75% with digital images and 83.5% with glass slides. Semiquantitative (0–3) density score agreement between trainees and trainer averaged 67% for glass slides and 62% for digital images.

Key Words: Biomarker, Biopsy, Colon, Digital imaging, Parkinson disease, Skin, Submandibular gland.

INTRODUCTION

Aggregation and/or post-translational modifications of α-synuclein (Asyn) are currently thought to be an essential link in the chain of events leading to Parkinson disease (PD). Therapies have been initiated against Asyn pathology but at present there is no biomarker with which to directly monitor any in vivo Asyn changes that might be induced. Multiple studies of unmodified Asyn in CSF have demonstrated only a small reduction in PD and a large overlap with clinical control subjects (1–3). The biofluids focus has shifted towards oligomers, truncations, other post-translational modifications and seeded aggregation assays. However, whether soluble Asyn species in CSF mirror intracellular pathologic Asyn is still unknown and there is still no large-scale confirmation of the utility of these approaches. Efforts to develop a specific imaging Asyn ligand have not yet been successful and it seems that this may be more difficult than it was with amyloid and tau tracers (4). Additionally, the biomarker search has been handicapped by the lack of an accurate diagnostic gold standard for PD, especially for early-stage disease, when neuropathology-confirmed studies have suggested (albeit with relatively small subject and clinician numbers) that the standard neurological examination may incorrectly categorize between 35% and 47% of subjects (5, 6). Dopaminergic imaging is likely to increase diagnostic accuracy but autopsy studies have found that approximately half of all misdiagnosed subjects have progressive supranuclear palsy, multiple system atrophy or corticobasal degeneration, all of which have a striatal dopaminergic deficit (5–8).

As many congenital neurological diseases manifest in the peripheral nervous system (PNS), and biopsies there yield definitive histological diagnoses for some of these, more than 10 years ago the possibility was raised of an Asyn pathology-based biopsy diagnosis and biomarker of PD. Reports of Lewy-like pathology in the PD PNS date back at least to the 1960s (9–11), and the development of Asyn immunohistochemical (IHC) methods in the late 1990s allowed this to be explored and mapped with much greater sensitivity and precision. Concurrently, the presence of Asyn pathology in the PD enteric nervous system became a candidate cause of the common gastrointestinal symptoms that often precede motor parkinsonism (12). Based on the presence of Asyn pathology in the stomach, the vagus nerve and its medullary dorsal motor nucleus, Braak and others hypothesized that causative Asyn molecular changes may begin after exposure to an exogenous agent followed by retrograde spread up the vagus into the CNS (13, 14). This provocative concept, while still lacking a convincing body of human autopsy evidence, stimulated an urgent search for PNS Asyn, with objectives that quickly extended beyond clinical correlation to its possible etiological and biomarker value. As colonoscopic cancer screening is now performed on most middle-aged people in first-world countries, there has been an intense focus on the colon, but other sites have also been scrutinized, including skin, stomach, esophagus, pharynx and salivary glands (15–24). The body of literature generated, however, has been so widely discordant as to threaten its credibility.

To address this, since 2013 the Michael J. Fox Foundation for Parkinson's Research (MJFF) has funded a series of meetings and projects, ultimately leading to the conclusion that blinded-panel histology evaluations with enforced blinding were necessary to overcome interlaboratory disagreements. Subsequently, 2 multi-investigator blinded-panel evaluations of Asyn pathology clearly established its selective, although inconsistent, presence in the PD colon and exclusion from controls (25, 26). These projects also identified precise morphological typing, sufficient tissue volume acquisition, and specialized reader training as additional crucial elements for future studies.

The MJFF is now funding the Systemic Synuclein Sampling Study (S4), a monitored observational study of individuals at early, middle and late clinical stages of PD, as well as normal control volunteers, each of whom are donating samples of cerebrospinal fluid, blood and saliva as well as biopsies of skin, colon, and submandibular gland (27). The study will determine whether biopsy sampling of Asyn tissue pathology is a practical, safe and useful undertaking, and whether tissue Asyn pathology correlates with biofluid measures taken from the same subjects. This report will summarize the development, selection and implementation of the methods to be applied in the biopsy component of S4.

MATERIALS AND METHODS

Tissue Processing

Fixation, Epitope Exposure, and Sectioning.

For all 3 biopsy sites, much of the pioneering Asyn IHC work was done on free-floating tissue preparations much thicker than the usual clinical pathology format of 3–8 μm. The Nantes group used thick whole-mounts of microdissected submucosa (19, 20) while the Braak-Del Tredici group (13–15), Arizona group (21) and the groups led by Freeman (28, 29) and Donadio (17, 30, 31) all have used free-floating sections ranging up to 100 μm. While these thick sections constitute a much larger tissue sample volume and allow the flexible and simultaneous investigation of multiple target molecules in 3 dimensions, especially with confocal laser fluorescence, the anticipated usage of the chosen S4 method as a biomarker in clinical trials makes demands that are best suited by standard-thickness, formalin-fixed, paraffin-embedded (FFPE), immunoperoxidase-stained sections. These can be archived without deterioration over a prolonged period of time as a permanent trial record, are easily shared, either as glass slides or scanned images, and are the standard format for automated immunostainers, allowing ease and reliability of replication, even at multiple centers. Other fixation methods, such as Zamboni's, have been favored by some laboratories, but no rigorous comparisons of fixatives for Asyn pathology have been published. In general, FFPE tissue often has less sensitivity for IHC (32–34), principally due to the high temperature or other aspects of paraffin infiltration that can result in masking of epitopes. Fortunately for PD studies, FFPE material, even with very prolonged fixation durations, has been shown to retain strong and selective immunoreactivity for Asyn pathology, especially in combination with appropriate epitope exposure pretreatments, such as formic acid, proteinase K or other proteases; the proteases also serve another useful purpose in that they digest unmodified Asyn that is abundant in normal PNS and CNS tissue (35).

For S4, biopsies are placed in standard plastic cassettes and fixed in commercially obtained 10% formalin (catalog number 23-245-685, Fisher Scientific, Chicago, IL) at 4°C overnight, while in overnight shipment to the Indiana University S4 Biorepository Core (see Supplementary Data Tissue Methods for full details of tissue processing). Upon arrival at the Biorepository Core, tissue cassettes are put through an automated tissue processor for further fixation, dehydration and paraffin infiltration (paraffin catalog number 13-374-10, Fisher Scientific). Following embedding, serial sections are cut at 4 μm through the entire specimen, mounted on Fisher brand positively charged slides (catalog # 12-550-15 Fisher Scientific), consecutively numbered and stored at room temperature. This is done to avoid having to resurface the paraffin block repeatedly when additional sections are needed, losing valuable and often limited biopsy tissue. The intent is to keep unstained slides for usage in future studies as needed. Preliminary studies have shown that storage of unstained FFPE slides of brain tissue for up to several years does not impair the density of pathological Asyn immunoreactivity, relative to newly cut sections from the same paraffin blocks (data not shown).

Basic Histology Quality Assessment With H&E-Stained Sections.

To assess for the suitability of S4 embedded tissue for IHC staining, and to confirm the presence of essential tissue components, 4 sections are taken through each paraffin-embedded block, equidistant through the tissue specimen, and stained with H&E, digitally scanned (Aperio, Leica Biosystems, Kassel, Germany) and transmitted to the Pathology Core lab at Banner Sun Health Research Institute. Tissue integrity, cutting or staining deficiencies and the presence of any incidental pathology, such as inflammation and neoplasm, are noted. An image analysis program (Zeiss AxioVision, Oberkochen, Germany) is used to manually trace and measure, on the slide with the largest tissue fragments, the cross-sectional area of tissue components considered essential for their possession of Asyn pathology. These critical tissue components are the colonic submucosa, the dermis of the skin and the glandular components (including stroma but excluding extraglandular tissue elements) of the submandibular gland. Based on past experience with submandibular gland biopsies (22, 23), a minimal cross-sectional area of 2 mm^2 of critical tissue components was defined as necessary for further IHC assessment of slides from that tissue cassette. For colon, the area of mucosa is also measured while for skin, additional areas measured include epidermis and hypodermis; these were not considered essential for S4 inclusion, however.

Choice of Epitope Exposure Method, Primary Antibody and Signal Development.

The great majority of studies of pathological Asyn have utilized antibodies raised against Asyn without post-translational modifications or Asyn phosphorylated at serine 129. At least some of the discrepant published results may be due to differences in the epitopes recognized, in addition to differences in the antigen retrieval procedure, the staining method and the detection protocol, all which are critical components of an IHC assay system. Antibodies raised against unmodified Asyn may recognize multiple forms of Asyn, including the large amounts that are normally expressed by healthy neural elements. In FFPE material, prolonged formalin fixation and hot paraffin embedding eliminates most normal Asyn immunoreactivity (35) and this may be further reduced or eliminated by digesting with proteinase K or other proteases, while still preserving the more concentrated and less-soluble pathological Asyn aggregates. Other approaches to the problem of confounding normal Asyn have used antibodies to purportedly pathology-specific, post-translational Asyn modifications such as phosphorylated (36), nitrosylated or truncated Asyn (37, 38). Although a clearly superior choice has not been conclusively proven, much evidence favors the usage of antibodies against Asyn phosphorylated at serine 129 (36, 39–42).

For S4, 2 earlier MJFF-sponsored, multicenter blinded-panel studies had tested multiple IHC methods for pathological Asyn on FFPE colonic tissue from biopsies (26) and autopsies (25). Several of these methods had achieved very good to

TABLE 1. Immunohistochemical Methods Tested

	Primary Antibody	Epitope Exposure	Signal Development
Nantes	p-synuclein monoclonal MJF-R13 (8-8) ab168381 Abcam* 1:10 000 (17)	Leica[†], Proteinase K for 15 minutes (Bond Enzyme Pretreatment Kit)	Leica[†], peroxidase blocking with Bond Enzyme Pretreatment Kit; mixed DAB Refine
RICM	a-synuclein monoclonal 5C12 (41) Prothena[‡] 1 μg/mL	Ventana[§] Protease 1 36°C, 12 minutes	Ventana Benchmark Ultra[§]; Optiview DAB IHC Detection Kit

*Abcam, Cambridge, UK.
[†]Leica Biosystems, Kassel, Germany.
[‡]Prothena Biosciences, Dublin, Ireland.
[§]Ventana Medical Systems, Tucson, Arizona.
p-synuclein = α-synuclein phosphorylated at serine 129; a-synuclein = α-synuclein unmodified form; DAB = 3,3′ di-aminobenzidine. All slides were counterstained with hematoxylin. See Supplementary Data Materials for full description.

excellent results, and all of these used antibodies against phosphorylated Asyn. All but one utilized automated staining machines. The method with the highest utility for identifying autopsied PD versus control colon, developed by the Nantes group (25), was chosen as 1 of 2 candidate methods for S4. This was compared, in a final study documented here, to a proof-of-concept method employing the 5C12 antibody against unmodified Asyn (Prothena Biosciences, Dublin, Ireland). This had been under development by the Roche Innovation Center Munich (RICM), using the automated Ventana BenchMark® platform, and was subsequently transferred to and analytically validated by Targos Molecular Pathology GmbH (Table 1; see Supplementary Data Tissue Processing for full details of the 5C12 method). Both methods employ protease-based epitope exposure and signal development utilizing peroxidase-mediated 3,3′-diaminobenzidine (DAB) chromogen precipitation (DAB obtained from Leica Biosystems, Kassel, Germany for the Nantes method and from Ventana Medical Systems, Tucson, AZ, for the method developed by RICM).

Selection, Training, and Role of Microscopic Tissue Readers

Readers were selected on the basis of possessing medical certification in neuropathology and were either American or Canadian board-certified. While any personnel with experience interpreting nervous system histology might be appropriate, neuropathologists have received highly specialized training, as well as formalized examination and certification, in the diagnostic evaluation of peripheral nerve biopsies. Additionally, the medical certification would be desirable if Asyn IHC evaluation is eventually utilized in clinical trials monitored by regulatory agencies. Three neuropathologists will independently view digital microscopic images of the S4 biopsies. One additional judge was chosen as an alternate. The "trainee" judges (DGM, CLW, JS, and JFC) were instructed by a "trainer" judge (TGB) with extensive experience in the evaluation of Asyn PNS pathology. The training consisted of a 1 day in-person session as well as subsequent independent blinded evaluation of a selection of photomicrographs, glass

slides and digitized glass slides. The instruction was principally directed at distinguishing specific from non-specific staining (for examples, see Figs. 1, 2). Building on the prior MJFF-sponsored studies in colon (25, 26), specific staining was explicitly defined as that consistent with a neuronal morphology and further supported by an appropriate anatomical context, eg a stained fiber within a nerve fascicle (nerve bundle) or closely applied to the abluminal surface of blood vessels. Double-staining studies have previously confirmed the neuronal identity of some types of presumptively specific staining morphologies (25, 43).

For S4, 3 slides from each cassette will be immunostained for pathological Asyn. Judges will view scanned digital images of immunostained slides (Aperio, Leica Biosystems). Digital images were found to be equivalent to glass slides in the methods development for S4 (see below). Judges will remain blinded, throughout S4, to subject group (PD vs healthy controls) as well as to the decisions or opinions of all of the other judges. The majority opinion of the 3 judges will be used for the primary analysis, ie sensitivity and specificity of Asyn pathology for the clinical diagnosis of PD versus control. This will be based on a binary decision as to whether the biopsy anatomical site is positive for Asyn pathology in at least 1 slide from any of the tissue cassettes from that subject. A semiquantitative density score (Fig. 3) derived from a grading template, based on the highest density observed within each anatomical site and microscopic compartment, will be assigned to each microscope slide. These will be correlated, in a secondary analysis, with clinical measures of PD severity, including Movement Disorders Society Unified Parkinson's Disease Rating Scale (MDS-UPDRS) scores. Additional measures of Asyn pathology density may be used in follow-up studies; these methods have not yet been chosen but will likely include fractional measures that employ total nerve fiber density as a denominator.

Final IHC Methods Comparison, Judge Training. and Digital Image vs Glass Slide Comparison

For the final comparison of the 2 IHC candidate S4 methods, autopsy tissue from the Arizona Study of Aging
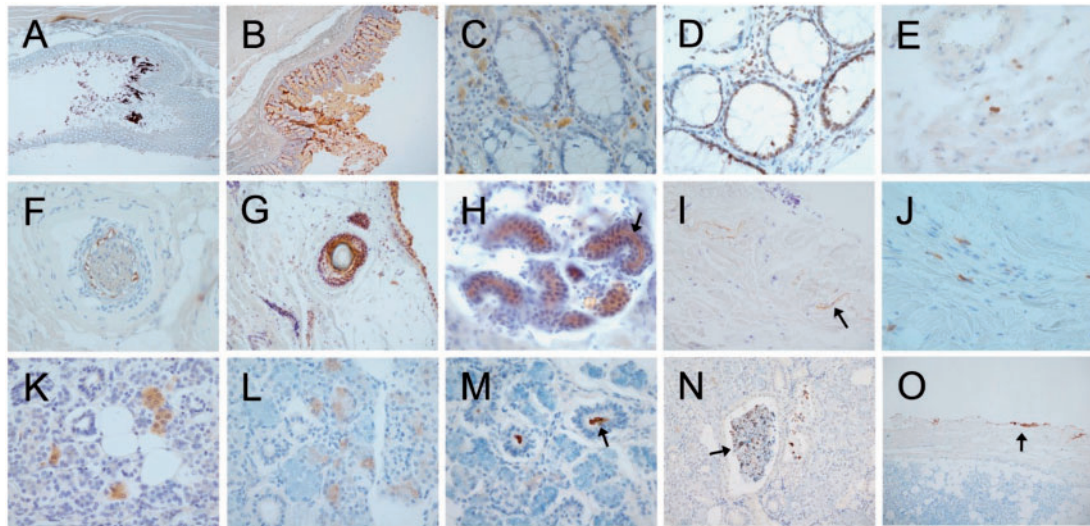
FIGURE 1. Photomicrographs of autopsy sections immunohistochemically stained for pathological Asyn by the 2 compared methods illustrating common types of non-specific staining. Specific versus non-specific staining morphologies have been defined by their neuronal or non-neuronal appearance and empirically by their differential presence in normal control subjects versus subjects with autopsy-confirmed PD or other Lewy body diseases. Immunoperoxidase reaction product is brown, the counterstain is blue. Panels **(A–E)** are of sigmoid colon, **(F–J)** of skin from scalp, and **(K–O)** of submandibular gland. Most staining features were seen with both staining methods. **(A, B)** Sigmoid colon stained with the 5C12 method **(A)** and the Nantes method **(B)**, showing non-specific DAB deposition on lumenal contents and within surface epithelial cells. **(C)** Mucosa of sigmoid colon, depicting frequent melanin-containing macrophages (melanosis coli) within the lamina propria, a relatively common non-specific finding (5C12 method). **(D)** Mucosa showing non-specific staining of epithelial cell nuclei; melanin-containing macrophages are also present in the lamina propria (5C12 method). **(E)** Macrophages non-specifically stained within the submucosa (5C12 method). **(F, G)** Non-specific staining of hair follicles (**[F]** with the 5C12 method, **[G]** with the Nantes method). Also seen in **(G)** are non-specifically stained melanocytes in the epidermis. **(H)** Sweat glands with non-specific staining of lumenal surfaces (arrow points to example; 5C12 method). **(I)** Collagen fibers (arrow points to an example) in the dermis, non-specifically taking up DAB (Nantes method). **(J)** Macrophages in the dermis with non-specific staining of cytoplasmic contents (5C12 method). **(K, L)** Diffuse, non-specific staining of cytoplasm of serous epithelial cells of submandibular gland (**[K]** with Nantes method, **[L]** with 5C12 method). **(M)** Non-specific staining of lumenal contents (arrow) of a duct within submandibular gland (5C12 method). **(N)** Non-specific DAB deposition on secretion (arrow) within a submandibular gland duct (5C12 method). **(O)** Non-specific DAB deposition along the edge of a submandibular gland biopsy (5C12 method).

and Neurodegenerative Disorders (AZSAND)/Banner Sun Health Research Institute Brain and Body Donation Program, www.brainandbodydonationprogram.org (44), was taken from all 3 anatomical sites, skin (from posterior scalp), colon and submandibular gland, from 6 subjects, including 3 with PD and 3 controls (Table 2). The PD subjects were deliberately selected on the basis of having had previously demonstrated higher densities of submandibular gland Asyn pathology. Two slides from each anatomical site were stained with each method and these, a total of 36 slides, were used by the trainer neuropathologist (TGB, "rater 1" in Table 3) and a second experienced neuropathologist (DGM, "rater 2" in Table 3) to compare the 2 finalist methods. Following this, the same set of slides were used for training and assessment of all trainee neuropathologists ("raters 1–4" in Table 4) and to compare results for glass slides versus digital images. All slide sets and digital images were separately coded so that judges were not aware of the subjects' diagnoses or of their own decisions for those subjects between regions or between glass slides and digital images.

RESULTS

Comparison of the 2 Candidate IHC Methods

The performance of the 2 finalist methods is summarized in Table 3. Although both provided clear definition of structures consistent with neuronal pathology (fibers and puncta consistent with axons and presynaptic terminals) in all 3 anatomical sites (Fig. 1), and both were 100% specific in that no false positive diagnostic decisions were made, the 5C12 method was more sensitive in skin (average of readers was 67% vs 33%), resulted in a higher density of positively stained structures (1.95 vs 1.40, mean score across all regions and both raters) and had a higher rate of score agreement between raters (55.6% vs 38.9%, absolute score agreement across all regions). On this basis, the 5C12 method was chosen for usage in the S4 study.

Comparison of the 4 Raters Using Both Glass Slides and Digital Images

The slides stained with the 5C12 method, and their corresponding digital images, were used to compare the 4
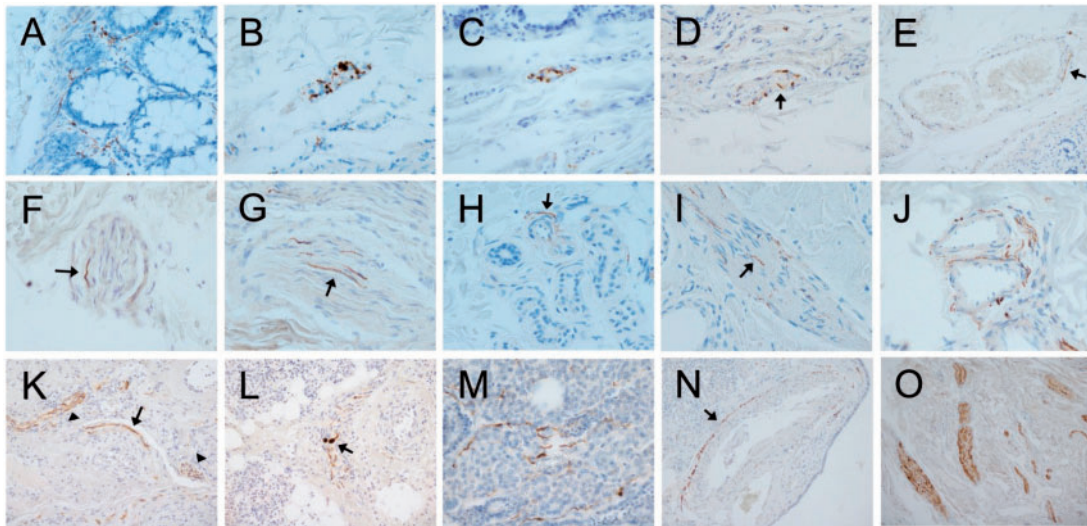
FIGURE 2. Photomicrographs of autopsy sections immunohistochemically stained for pathological Asyn by the 2 compared methods illustrating common types of presumptively specific staining. Specific versus non-specific staining morphologies have been defined by their neuronal or non-neuronal appearance and empirically by their differential presence in normal control subjects versus subjects with autopsy-confirmed PD or other Lewy body diseases. Immunoperoxidase reaction product is brown, the counterstain is blue. Panels **(A–E)** are of sigmoid colon, **(F–J)** of skin from scalp, and **(K–O)** of submandibular gland. Most staining features were seen with both staining methods. **(A)** Several "beaded" fibers, consistent with axons, within the lamina propria (5C12 method). **(B, C)** Short fibers and puncta, the former consistent with axons, the latter consistent with presynaptic terminals or dystrophic neurites, within a ganglion of the submucosal plexus (**[B]** with the 5C12 method, **[C]** with the Nantes method). **(D)** Short perivascular fibers (arrow) and puncta, consistent with axons, within the submucosa (5C12 method). **(E)** Longer fiber, consistent with an axon, closely applied to the abluminal surface of a blood vessel within the submucosa (arrow; 5C12 method). **(F, G)** Fibers consistent with axons (arrows point to examples), within small nerve fascicles in the dermis (**[F]** with Nantes method, **[G]** with 5C12 method). **(H)** Fiber consistent with axon (arrow) applied to the ablumenal surface of a small blood vessel within a cluster of dermal sweat glands (5C12 method). **(I)** Fine fibers consistent with axons (arrow points to an example) on the surface of an arrector pili muscle in the dermis (5C12 method). **(J)** Multiple fibers applied to the ablumenal surfaces of dermal blood vessels; fibers running in parallel adjacent to 1 vessel are within a small nerve fascicle (5C12 method). **(K)** Long fibers (arrow) applied to the ablumenal surface of a blood vessel within the submandibular gland (Nantes method). Also seen are fibers running in parallel within a small nerve fascicle (arrowhead on left) and puncta presumptively representing cross-sectioned axons within a nerve fascicle (arrowhead on right). **(L)** Fibers running in parallel within a small submandibular gland nerve fascicle (Nantes method); 2 fibers have focal enlargements, consistent with dystrophic change (arrow). **(M)** Several fibers consistent with axons amongst serous epithelial cells (5C12 method). **(N)** Long fiber(s) closely applied to the ablumenal surface (arrow) of an arteriole within the submandibular gland (5C12 method). **(O)** Several large nerve fascicles within the stroma of the submandibular gland, each with numerous immunoperoxidase-stained fibers consistent with axons (5C12 method).

"trainee" raters to the "trainer" rater and to compare the performance of reads in glass and digital formats (Table 4). In terms of specificity, there were almost no differences between raters, with either glass slides or digital images, as specificity was 100% with all readers in all anatomical regions except for 1 reader who had 1 false positive decision with the digital images. In terms of sensitivity, in submandibular gland and colon, readers were almost all concurrent at 100% except for a single reader who had 1 false negative decision in the colon digital images. Sensitivity for skin was lower than for the other anatomical regions. Two of the 4 raters for glass slides, and 3 of the 4 raters for digital images, had single false negative decisions in all cases recording the same PD subject as falsely negative. The aggregate of all density scores were slightly higher on glass slides for trainee raters (overall mean 2.05 vs 1.85; p = 0.52), while for the trainer they were slightly higher for the digital images (2.1 vs 2.2). In terms of agreement on density scores between the trainer and trainee raters, the overall agreement was slightly greater with glass slides than with digital images (67% vs 62%, Table 5). The variability of the grouped trainees' agreement percentages with the trainer was equivalent between glass and digital images (SDs of 28.0 and 31.6, respectively).

On the basis of the above comparisons, a decision was made to use digital images for S4 histology judging. The usage of digital images not only reduces the risk of loss or damage to slides but also allows for simultaneous independent assessment of the histology and consequently reduced time to have completed assessments done by all 3 judges.

DISCUSSION

Biomarker efforts for PD have recently extended to peripheral tissue biopsy measures of Asyn pathology. Two MJFF-sponsored multicenter studies of colon Asyn have indicated that prior replication failures amongst a number of single

centers were very likely due to combinations of insufficient tissue volume, attribution of specificity to non-neuronal morphologies or inadequate training and experience of histology judges (25, 26). These insights have guided the development of histology methods for the S4 study, as described here.

The single most critical principle has been the definition of specific staining as that which is consistent with a neuronal morphology. While it is still possible that peripheral synucleinopathy in PD may be found in other cell types, it seems more likely that, as in other neurological disorders that may be

diagnosed by peripheral biopsy, the characteristic pathology will be restricted to neural tissue elements.

The comparison of 2 IHC methods, developed by the RICM and Nantes groups, somewhat surprisingly found the former method, utilizing the 5C12 antibody against unmodified Asyn, as superior in sensitivity to the monoclonal used by the Nantes group, against Asyn phosphorylated at serine 129, while having identical specificity. The Nantes method had the best performance of several antibodies in the recent MJFF-sponsored multicenter study of autopsy colon Asyn pathology (25). The method developed at RICM (see Supplementary Data Methods section) utilizes the 5C12 antibody against unmodified Asyn, directed against amino acids 120–140 (45). While the phosphorylated form of Asyn is thought to be highly specific for pathological deposition in Lewy pathology, as mentioned, antibodies against unmodified Asyn may also be employed, especially with FFPE tissue, as prolonged or heated formalin-fixation and hot paraffin-embedding often eliminates most normal Asyn immunoreactivity and pretreatment with proteinase K or other proteases appears to eliminate any that remains, while preserving the pathological Asyn aggregates
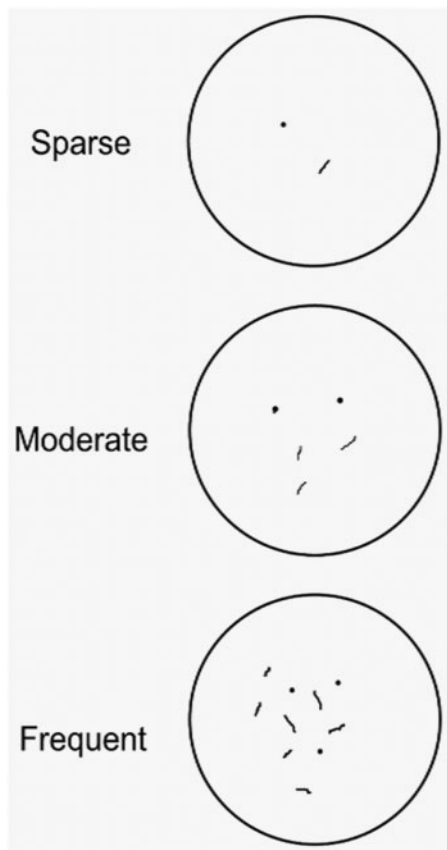

FIGURE 3. Template used by judges to grade the density of presumptively specific fibers and puncta representing axons and presynaptic terminals. Depicted is the appearance with a 40× microscope objective and 10× ocular magnification.

TABLE 3. Diagnostic Performance Using Glass Slides for the 2 Tested Methods, With 2 Independent Blinded Raters, Using Any Score >0 as the Definition of PD Diagnosis

Rater	Sensitivity %			Specificity %			Density/ Agreement		
Anatomical Site	SMG	COL	SKIN	SMG	COL	SKIN	SMG	COL	SKIN
5C12									
Rater 1	100	100	67	100	100	100	3	1.5	1.8
Rater 2	100	100	67	100	100	100	3	1.2	1.2
Both (mean)	100	100	67	100	100	100	3	1.35	1.5
Agreement % (PD)							100	16.7	50
Nantes									
Rater 1	100	100	33	100	100	100	2.83	1.9	0.08
Rater 2	100	100	33	100	100	100	2.5	1.0	0.08
Both (mean)	100	100	33	100	100	100	2.66	1.45	0.08
Agreement % (PD)							66.6	50	0

The column headed by "Density/Agreement" lists the mean density scores (only PD scores were used; scores for subregions were averaged) for each rater. Agreement is the percentage of scores that were identical for the 2 raters.

TABLE 2. Characteristics of Study Subjects

	Age Mean (SD)	Gender (M: F)	PMI Mean (SD)	Clinical Symptoms Years Mean (SD)	UPDRS Mean (SD)	Unified Lewy Stage Median	Lewy CNS Total Score Mean (SD)
PD (n = 3)	81.0 (6.2)	1: 0	3.19 (1.1)	14.3 (11.2)	40.7 (17.9)	IV	29.7 (0.6)
Control (n = 3)	84.0 (7.0)	1: 0	3.36 (1.9)	NA	9 (8.5)	NA	NA

PMI = postmortem interval in hours; clinical symptoms = symptom duration; UPDRS = last motor score prior to death on the Unified Parkinson's Disease Rating Scale (44); Unified Lewy Stage = brain stage of LTS according to the Unified Staging System for Lewy Body Disorders (39); Lewy CNS Total Score = mean summary score of LTS density in 10 standard brain regions (39).

TABLE 4. Comparison of Blinded Trainee Performance Versus Blinded Trainer Performance, On Both Glass Slides and Digital Images, Using Slides Stained With the 5C12 Method

Rater	Sensitivity %			Specificity %			Density		
Anatomical Site	SMG	COL	SKIN	SMG	COL	SKIN	SMG	COL	SKIN
Glass slides									
Trainee 1	100	100	100	100	100	100	3	1.75	2.25
Trainee 2	100	100	67	100	100	100	3	1.2	1.2
Trainee 3	100	100	100	100	100	100	3	1.7	1.3
Trainee 4	100	100	67	100	100	100	3	1.6	1.6
All trainees (mean)	100	100	83.5	100	100	100	3	1.6	1.6
Trainer	100	100	67	100	100	100	3	1.5	1.8
Digital images									
Trainee 1	100	100	67	100	100	100	3	1.3	1.4
Trainee 2	100	67*	100	100	67*	100	2.3	1.4	1.25
Trainee 3	100	100	67	100	100	100	3	1.6	1.1
Trainee 4	100	100	67	100	100	100	3	1.25	1.6
All trainees (mean)	100	92	75	100	92	100	2.8	1.4	1.3
Trainer	100	100	100	100	100	100	3	1.5	2.1

*Corrected on blinded re-read with corrected sensitivity and specificity of 100%, second read data used for density calculations.

TABLE 5. Agreement Percentage for Each of the 4 Trainees Versus the Trainer, for Density Scores on Glass Slides and Digital Images and Each of the 3 Anatomical Areas, for PD Cases Only, Stained With the 5C12 Method

	Trainee 1	Trainee 2	Trainee 3	Trainee 4	All Trainees
Glass					
SMG	100	100	100	100	100
COL	50	17	80	50	49
SKIN	42	50	60	58	52.5
Mean	64	56	80	69	67
Digital					
SMG	100	33	100	100	83
COL	67	58	83	83	73
SKIN	25	25	17	50	29
Mean	64	39	67	78	62

Agreement is the percentage of scores that were identical between the trainee and trainer.

(35). This process needs to be tightly controlled and standardized, however, to avoid also digesting pathological Asyn and causing deleterious effects on the tissue specimen. As an antibody against unmodified Asyn had also proven superior for identifying brain Asyn pathology, in an earlier multicenter study (35), to several others including antibodies against phosphorylated Asyn, it is possible that Lewy pathology is only partially composed of phosphorylated Asyn (46) and that more epitopes are available for antibodies against unmodified

Asyn, allowing better sensitivity. However, the differences between the highest-performing methods, both in prior studies (25, 35) and in the study reported here, were not large.

Although this blinded-panel assessment of Asyn pathology was intended only to allow comparison of Asyn IHC methods and digital imaging versus glass slides, the density and prevalence ranking of the 3 anatomical sites, ie submandibular gland, colon, skin, confirms that established by a much larger autopsy study (21). The study also suggests that reading of digital slide images will be suitable for future neuropathology studies, confirming a similar conclusion reached by a group assessing Alzheimer disease histopathology (47).

The most immediate usefulness of biopsies for peripheral tissue Asyn pathology, should sensitivity and specificity be sufficiently high in typical clinical trial PD patients, would be to improve subject selection for inclusion in trials of Asyn-targeting agents in early-stage PD. Improving the diagnostic accuracy with biopsy would result in more PD subjects and fewer non-PD subjects being included in trials, allowing trials to be performed with smaller subject numbers and less cost. Although it is possible that subjects with multiple system atrophy (MSA) might have positive peripheral biopsies for Asyn pathology, their inadvertent inclusion in a clinical trial would most probably not significantly affect any measured outcomes as MSA is much less common than PD; multiple system atrophy cases total only 2% of PD cases in the AZSAND autopsy series (44).

Even if not used for subject selection, biopsy data could be used to separate subjects into 2 groups, the positives and the negatives, each with possibly different disease characteristics, including perhaps a higher or lower probability of response or toxicity to a new treatment, allowing differential analyses that might save an otherwise negative trial. A stratified analysis such as this might also be applied to biomarkers being evaluated in parallel to biopsy, as peripheral tissue evidence of Asyn pathology may prove to be a serviceable surrogate for autopsy validation.

Perhaps the greatest promise for biopsies is as a direct measure of the disease-associated molecular pathology. At present there is no way to directly monitor the response to anti-synucleinopathy agents, such as Asyn-directed immunotherapy. Repeat biopsies separated in time would provide a means for this, provided that the natural history of peripheral Asyn pathology is to increase or remain stable over time. Orimo and colleagues have suggested that peripheral Asyn pathology peaks early in disease and then progressively disappears as nerve fibers die back (48). Fujishiro, Dickson and colleagues, however, have published evidence that cardiac Asyn pathology increases with disease duration and severity (49). Beyond S4, the next priority would be to establish, with serial biopsies over time, whether Asyn peripheral pathology can be repeatedly and reproducibly measured in the same subjects. Eventual autopsy of biopsied subjects would relate biopsy findings to final diagnosis and CNS Asyn stage (39).

If the utility of detecting peripheral, pathological Asyn in tissue biopsies for discriminating PD patients from corresponding non-PD controls can be demonstrated in this and

other clinical studies, the further development of this method or an equivalent method into a diagnostic solution for PD clinical decision making could be envisioned. This may ultimately lead to a novel early diagnostic test or a companion diagnostic assay to accompany anti-synucleinopathy treatments currently under development. To this end, the current proof-of-concept assays will need to be optimized and advanced further into an in vitro diagnostic device whose design and manufacturing process have been rigorously verified in elaborate analytical studies to confirm assay precision and robustness as well as a reproducible manufacturing procedure.

ACKNOWLEDGMENTS

REFERENCES

1. Atik A, Stewart T, Zhang J. Alpha-synuclein as a biomarker for Parkinson's disease. Brain Pathol 2016;26:410–8
2. Simonsen AH, Kuiperij B, El-Agnaf OM, et al. The utility of alpha-synuclein as biofluid marker in neurodegenerative diseases: A systematic review of the literature. Biomarkers Med 2016;10:19–34
3. Mollenhauer B, Parnetti L, Rektorova I, et al. Biological confounders for the values of cerebrospinal fluid proteins in Parkinson's disease and related disorders. J Neurochem 2016;139 (Suppl. 1):290–317
4. Catafau AM, Bullich S. Non-amyloid PET imaging biomarkers for neurodegeneration: Focus on tau, alpha-synuclein and neuroinflamation. Curr Alzheimer Res 2016;14:169–77
5. Rajput AH, Rozdilsky B, Rajput A. Accuracy of clinical diagnosis in parkinsonism: a prospective study. Can J Neurol Sci 1991;18:275–8
6. Adler CH, Beach TG, Hentz JG, et al. Low clinical diagnostic accuracy of early vs advanced Parkinson disease: Clinicopathologic study. Neurology 2014;83:406–12
7. Stoessl AJ, Halliday GM. DAT-SPECT diagnoses dopamine depletion, but not PD. Mov Disord 2014;29:1705–6
8. Hughes AJ, Daniel SE, Kilford L, et al. Accuracy of clinical diagnosis of idiopathic Parkinson's disease: A clinico-pathological study of 100 cases. J Neurol Neurosurg Psychiatry 1992;55:181–4
9. den Hartog Jager WA, Bethlem J. The distribution of Lewy bodies in the central and autonomic nervous systems in idiopathic paralysis agitans. J Neurol Neurosurg Psychiatry 1960;23:283–90
10. Qualman SJ, Haupt HM, Yang P, et al. Esophageal Lewy bodies associated with ganglion cell loss in achalasia. Similarity to Parkinson's disease. Gastroenterology 1984;87:848–56
11. Wakabayashi K, Takahashi H, Takeda S, et al. Parkinson's disease: The presence of Lewy bodies in Auerbach's and Meissner's plexuses. Acta Neuropathol 1988;76:217–21
12. Adler CH, Beach TG. Neuropathological basis of nonmotor manifestations of Parkinson's disease. Mov Disord 2016;31:1114–9
13. Braak H, de Vos RA, Bohl J, et al. Gastric alpha-synuclein immunoreactive inclusions in Meissner's and Auerbach's plexuses in cases staged for Parkinson's disease-related brain pathology. Neurosci Lett 2006;396:67–72
14. Braak H, Rub U, Gai WP, et al. Idiopathic Parkinson's disease: Possible routes by which vulnerable neuronal types may be subject to neuroinvasion by an unknown pathogen. J Neural Transm 2003;110:517–36
15. Del Tredici K, Hawkes CH, Ghebremedhin E, et al. Lewy pathology in the submandibular gland of individuals with incidental Lewy body disease and sporadic Parkinson's disease. Acta Neuropathol 2010;119:703–13
16. Lee JM, Derkinderen P, Kordower JH, et al. The search for a peripheral biopsy indicator of alpha-synuclein pathology for Parkinson disease. J Neuropathol Exp Neurol 2017;76:2–15
17. Antelmi E, Donadio V, Incensi A, et al. Skin nerve phosphorylated alpha-synuclein deposits in idiopathic REM sleep behavior disorder. Neurology 2017;88:2128–31
18. Doppler K, Jentschke HM, Schulmeyer L, et al. Dermal phospho-alpha-synuclein deposits confirm REM sleep behaviour disorder as prodromal Parkinson's disease. Acta Neuropathol 2017;133:535–45
19. Pouclet H, Lebouvier T, Coron E, et al. A comparison between colonic submucosa and mucosa to detect Lewy pathology in Parkinson's disease. Neurogastroenterol Motil 2012;24:e202–5
20. Pouclet H, Lebouvier T, Coron E, et al. A comparison between rectal and colonic biopsies to detect Lewy pathology in Parkinson's disease. Neurobiol Dis 2012;45:305–9
21. Beach TG, Adler CH, Sue LI, et al. Multi-organ distribution of phosphorylated alpha-synuclein histopathology in subjects with Lewy body disorders. Acta Neuropathol 2010;119:689–702
22. Adler CH, Dugger BN, Hinni ML, et al. Submandibular gland needle biopsy for the diagnosis of Parkinson disease. Neurology 2014;82:858–64
23. Adler CH, Dugger BN, Hentz JG, et al. Peripheral synucleinopathy in early Parkinson's eisease: Submandibular gland needle biopsy findings. Mov Disord 2016;31:250–6
24. Vilas D, Iranzo A, Tolosa E, et al. Assessment of alpha-synuclein in submandibular glands of patients with idiopathic rapid-eye-movement sleep behaviour disorder: A case-control study. Lancet Neurol 2016;15:708–18
25. Beach TG, Corbille AG, Letournel F, et al. Multicenter assessment of immunohistochemical methods for pathological alpha-synuclein in autopsied sigmoid colon of Parkinson's disease and control subjects. J Parkinson's Dis 2016;6:761–70
26. Corbille AG, Letournel F, Kordower JH, et al. Evaluation of alpha-synuclein immunohistochemical methods for the detection of Lewy-type synucleinopathy in gastrointestinal biopsies. Acta Neuropathol Commun 2016;4:35
27. Visanji NP, Mollenhauer B, Beach TG, et al. The Systemic synuclein sampling study: Toward a biomarker for Parkinson's disease. Biomark Med 2017;11:359–68

28. Wang N, Gibbons CH, Lafo J, et al. α-Synuclein in cutaneous autonomic nerves. Neurology 2013;81:1604–10
29. Gibbons CH, Garcia J, Wang N, et al. The diagnostic discrimination of cutaneous α-synuclein deposition in Parkinson disease. Neurology 2016;87:505–12
30. Donadio V, Incensi A, Leta V, et al. Skin nerve α-synuclein deposits: A biomarker for idiopathic Parkinson disease. Neurology 2014;82:1362–9
31. Donadio V, Incensi A, Piccinini C, et al. Skin nerve misfolded alpha-synuclein in pure autonomic failure and Parkinson disease. Ann Neurol 2016;79:306–16
32. Klosen P, Maessen X, van den Bosch de Aguilar P. PEG embedding for immunocytochemistry: Application to the analysis of immunoreactivity loss during histological processing. J Histochem Cytochem 1993;41:455–63
33. Arnold MM, Srivastava S, Fredenburgh J. Effects of fixation and tissue processing on immunohistochemical demonstration of specific antigens. Biotech Histochem 1996;71:224–30
34. Leong AS, Gilham PN. The effects of progressive formaldehyde fixation on the preservation of tissue antigens. Pathology 1989;21:266–8
35. Beach TG, White CL, Hamilton RL, et al. Evaluation of alpha-synuclein immunohistochemical methods used by invited experts. Acta Neuropathol 2008;116:277–88
36. Fujiwara H, Hasegawa M, Dohmae N, et al. alpha-Synuclein is phosphorylated in synucleinopathy lesions. Nat Cell Biol 2002;4:160–4
37. Baba M, Nakajo S, Tu PH, et al. Aggregation of alpha-synuclein in Lewy bodies of sporadic Parkinson's disease and dementia with Lewy bodies. Am J Pathol 1998;152:879–84
38. Xuan Q, Zhang YX, Liu DG, et al. Post-translational modifications of alpha-synuclein contribute to neurodegeneration in the colon of elderly individuals. Mol Med Rep 2016;13:5077–83
39. Beach TG, Adler CH, Lue L, et al. Unified staging system for Lewy body disorders: Correlation with nigrostriatal degeneration, cognitive impairment and motor dysfunction. Acta Neuropathol 2009;117:613–34
40. Beach TG, Carew J, Serrano G, et al. Phosphorylated alpha-synuclein-immunoreactive retinal neuronal elements in Parkinson's disease subjects. Neurosci Lett 2014;571:34–8
41. Obi K, Akiyama H, Kondo H, et al. Relationship of phosphorylated alpha-synuclein and tau accumulation to Abeta deposition in the cerebral cortex of dementia with Lewy bodies. Exp Neurol 2008;210:409–20
42. Walker DG, Lue LF, Adler CH, et al. Changes in properties of serine 129 phosphorylated alpha-synuclein with progression of Lewy-type histopathology in human brains. Exp Neurol 2013;240:190–204
43. Beach TG, Adler CH, Serrano G, et al. Prevalence of submandibular gland synucleinopathy in Parkinson's disease, dementia with Lewy bodies and other Lewy body disorders. J Parkinsons Dis 2016;6:153–63
44. Beach TG, Adler CH, Sue LI, et al. Arizona study of aging and neurodegenerative disorders and brain and body donation program. Neuropathology 2015;35:354–89
45. Anderson JP, Walker DE, Goldstein JM, et al. Phosphorylation of Ser-129 is the dominant pathological modification of alpha-synuclein in familial and sporadic Lewy body disease. J Biol Chem 2006;281:29739–52
46. Kellie JF, Higgs RE, Ryder JW, et al. Quantitative measurement of intact alpha-synuclein proteoforms from post-mortem control and Parkinson's disease brain tissue by intact protein mass spectrometry. Sci Rep 2014;4:5797
47. Montine TJ, Monsell SE, Beach TG, et al. Multisite assessment of NIA-AA guidelines for the neuropathologic evaluation of Alzheimer's disease. Alzheimers Dement 2016;12:164–9
48. Orimo S, Uchihara T, Nakamura A, et al. Axonal alpha-synuclein aggregates herald cen tripetal degeneration of cardiac sympathetic nerve in Parkinson's disease. Brain 2008;131:642–50
49. Fujishiro H, Frigerio R, Burnett M, et al. Cardiac sympathetic denervation correlates with clinical and pathologic stages of Parkinson's disease. Mov Disord 2008;23:1085–92

APPENDIX: SYSTEMIC SYNUCLEIN SAMPLING STUDY (S4) ADDITIONAL AUTHORS

Lindsey Guilmette, BS, CRA, David Russell, MD, PhD, Chaucer Noyes-Lloyd, RN, Colleen Mitchell, BS, Danielle Smith, BS, CCRP, Madeline Potter, BA, CCRP, Rose Case, BS, David Lott, MD, Amy Duffy, CCRP, Penelope Hogarth, MD, Madeline Cresswell, BS, Rizwan Akhtar, MD, Rachael Purri, BA, Amy Amara, MD, PhD, Courtney Blair, MA, Ali Keshavarzian, MD, Connie Marras, MD, PhD, Naomi Visanji, PhD, Brandon Rothberg, BA, and Vikash Oza, MD

From the Institute for Neurodegenerative Disorders, New Haven, Connecticut (LG, DR, CN-L); Department of Medical and Molecular Genetics, Indiana University, Indianapolis, Indiana (CM, DS, MP, RC); Department of Neurology, Mayo Clinic, Phoenix, Arizona (DL, AD); Department of Molecular and Medical Genetics, Oregon Health and Science University, Portland, Oregon (PH); Oregon Clinical and Translational Research Institute, Oregon Health and Science University, Portland, Oregon (MC); Department of Neurology, University of Pennsylvania, Philadelphia, Pennsylvania (RA, RP); Department of Neurology, University of Alabama at Birmingham, Birmingham, Alabama (AA, CB); Department of Gastroenterology, Rush University, Chicago, Illinois (AK); Department of Neurology, Toronto Western Hospital Movement Disorders Centre, Toronto, Canada (CM, NV, BR); The Ronald O. Perelman Department of Dermatology, School of Medicine, New York University, New York, New York (VO).